

NUMERICAL SIMULATION OF THE LAMINAR HYDROGEN FLAME IN THE PRESENCE OF A QUENCHING MESH

Kudriakov S.¹, Studer E.², Bin C.³

¹CEA/LTMF, 91191, Gif-sur-Yvette, France, skudriakov@cea.fr,

²CEA/LTMF, 91191, Gif-sur-Yvette, France, etienne.studer@cea.fr,

³Nuclear Power Institute of China, Chengdu, China, toyarmybin@gmail.com.

ABSTRACT

Recent studies of J.H. Song et al. [1] have been concentrated on mitigation measures against hydrogen risk. The authors have proposed installation of quenching meshes between compartments or around the essential equipment in order to contain hydrogen flames. Preliminary tests were conducted which demonstrated the possibility of flame extinction using metallic meshes of specific size.

Considerable amount of numerical and theoretical work on flame quenching phenomenon has been performed in the second half of the last century and several techniques and models have been proposed to predict the quenching phenomenon of the laminar flame system (see for example [2] and references therein). Most of these models appreciated the importance of heat loss to the surroundings as a primary cause of extinguishment, in particular, the heat transfer by conduction to the containing wall. The supporting simulations predict flame-quenching structure either between parallel plates (quenching distance) or inside a tube of a certain diameter (quenching diameter).

In the present study the flame quenching is investigated assuming the laminar hydrogen flame propagating towards a quenching mesh using two-dimensional configuration and the earlier developed models. It is shown that due to a heat loss to a metallic grid the flame can be quenched numerically.

1 Introduction

During certain postulated accidents, hydrogen may be released or generated into nuclear reactor containments or, more generally, into industrial units where hydrogen risk analysis has to be taken into account. Depending on the local concentration and/or the presence and activation of mitigation measures or devices, hydrogen may burn following different modes (diffusion flames, local or global deflagration, accelerated flames, detonation), or may not burn at all. It is therefore very important to predict the interaction of combustion front with the mitigation measures or devices. The mitigation measures/devices taken under consideration in order to counter the hydrogen risk include Passive Autocatalytic Recombiner (PAR), sprays, igniters, etc.

The installation of a quenching mesh between the compartments or the enclosure of the equipment by a quenching mesh has been suggested as a measure to prevent the flame propagation among compartments and/or to maintain equipment survivability [1].

Considerable amount of numerical and theoretical work on flame quenching phenomenon has been performed in the second half of the last century and several techniques and models have been proposed to predict the quenching phenomenon of the laminar flame system (see

for example [2] and references therein). Most of these models appreciated the importance of heat loss to the surroundings as a primary cause of extinguishment, in particular, the heat transfer by conduction to the containing wall. The supporting simulations predict flame-quenching structure either between parallel plates (quenching distance) or inside a tube of a certain diameter (quenching diameter).

The quenching distance for hydrogen-air stoichiometric mixture often cited in the literature is about 0.6 mm [3]. However it has been established that an explosion may be transmitted through the gap between two plane surfaces even when the gap is less than the quenching distance. Fortunately, there is a lower limit to the size of gap through which an explosion may be transmitted, which depends on the geometry of the gap and on the nature of the inflammable mixture. Experimental values of this lower limit, or critical gap size, called “Maximum Experimental Safe Gap” (MESG) are available in literature on industrial safety [4], and they are generally less than a quenching distances. For example, for hydrogen, the value of MESG is only about 0.3 mm.

An experiment to determine the quenching distance for hydrogen gas under the severe accident conditions of nuclear power plants was performed [5], where the effect of the steam addition and initial pressure on the quenching distance were also experimentally investigated. It showed that a quenching distance of 0.3 mm for hydrogen gas, which coincides with the value of MESG described above, was suitable for an application in nuclear power plants.

The purpose of the present study is to model hydrogen-air combustion front quenching assuming the laminar hydrogen flame propagating towards a quenching mesh using two-dimensional configuration and the earlier developed models.

2 Problem Description

In this study we shall model in two-dimensions a laminar flame quenching by a metallic mesh of size 0.3 mm (this value is taken for wire diameter as well as the inter-wire distance) using the CAST3M code [6]. The following assumptions on initial and boundary conditions are made throughout this study:

- stoichiometric hydrogen-air mixture;
- initial values for temperature and pressure are $T_0 = 300$ K, $P_0 = 1$ atm;
- metallic wire temperature is constant in time and equal to the ambient temperature, 300 K.

The last statement appears to be restrictive at first glance. Let us estimate a thermal penetration time corresponding to the wire radius, i.e. $r = 1.5 \times 10^{-4}$ m. Taking for the Fourier number the value $Fo = \lambda \Delta t / (\rho C_p r^2) = 1$ it follows that $\Delta t \approx 6$ ms. During 0.1 ms (this time scale corresponds to the length scale of $r = 0.15$ mm, and velocity scale of 1.5 m/s), the penetration distance is only about 0.02 mm, which is $\frac{1}{15}$ of wire diameter.

We consider a laminar flame, initially parallel to the plane of the mesh and moving towards it. In two-dimensional geometry the mesh is represented by a series of circles of diameter $D = 0.3$ mm, and we can exploit the symmetry of the problem considering for computational purposes only the part of the domain bounded by red solid line (see Fig. 1)

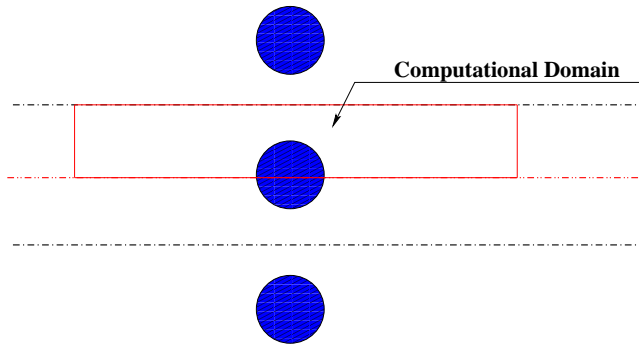


Figure 1: Sketch of the problem. The metallic cylinders are represented by blue circles.

3 Physical modelling

In this section we describe the governing equations for reactive fluid flow and the combustion kinetics which allows to model flame quenching. Single-step Arrhenius rate is used and radiation loss is neglected throughout the analysis.

3.1 Governing Equations.

The flow of a reactive Newtonian multi-component fluid of N species is governed by the Navier-Stokes equations which express the conservation of total mass (without source of mass), the mass conservation for species k ($k = 1, \dots, N - 1$), conservation of momentum and energy [7],

$$\frac{\partial \rho}{\partial t} + \vec{\nabla} \cdot (\rho \vec{u}) = 0 \quad (1)$$

$$\frac{\partial \rho Y_k}{\partial t} + \vec{\nabla} \cdot (\rho (\vec{u} + \vec{V}_k) Y_k) = \dot{\omega}_k \quad (2)$$

$$\frac{\partial \rho \vec{u}}{\partial t} + \vec{\nabla} \cdot (\rho \vec{u} \otimes \vec{u} + P \mathbf{I}) = \vec{\nabla} \cdot \underline{\underline{\tau}} + \rho \vec{g} \quad (3)$$

$$\frac{\partial \rho e_{tot}}{\partial t} + \vec{\nabla} \cdot (\rho \vec{u} h_{tot}) = \vec{\nabla} \cdot (\underline{\underline{\tau}} \cdot \vec{u} - \vec{q}) + \rho \vec{g} \cdot \vec{u} - \dot{\omega}_T \quad (4)$$

Hereafter we shall neglect the contributions due to gravity. The mass fractions Y_k , ($k = 1, \dots, N$), the species density ρ_k and the mixture density ρ are related by:

$$Y_k = \frac{\rho_k}{\rho} \quad (5)$$

and Fick's law is used for the diffusion velocity \vec{V}_k of species k

$$V_{k,i} Y_k = -D_k \frac{\partial Y_k}{\partial x_i} \quad (6)$$

with D_k being the diffusion coefficient of species k into the mixture. Following Stokes' hypothesis, the viscous shear stress tensor $\underline{\underline{\tau}}$ is given by:

$$\tau_{ij} = \mu \left(\frac{\partial u_i}{\partial x_j} + \frac{\partial u_j}{\partial x_i} - \frac{2}{3} \delta_{ij} \vec{\nabla} \cdot \vec{u} \right) \quad (7)$$

and the energy flux is

$$q_i = -\lambda \frac{\partial T}{\partial x_i} - \rho \sum_{k=1}^N h_k D_k \frac{\partial Y_k}{\partial x_i} \quad (8)$$

This flux includes a heat diffusion term expressed by Fourier's law and a second term associated with the diffusion of species with different enthalpies. Soret (molecular species diffusion due to temperature gradients) and Dufour (heat flux due to species mass fraction gradient) effects are neglected here.

The standard notations are used for the specific total enthalpy, h_{tot} , specific total energy, e_{tot} , and specific internal enthalpy for the species k ($k = 1, \dots, N$), h_k :

$$h_{tot} = e_{tot} + \frac{P}{\rho}, \quad e_{tot} = \int_0^T c_v dT' + \frac{1}{2} \vec{u} \cdot \vec{u}, \quad h_k = \int_0^T c_{pk} dT'. \quad (9)$$

The source term due to combustion in the energy equation is

$$\dot{\omega}_T = \sum_{k=1}^N \Delta h_{f,k} \dot{\omega}_k \quad (10)$$

with $\Delta h_{f,k}$ being the mass formation enthalpy of species k at the reference temperature $T = 0$ K. The data for $\Delta h_{f,k}$ and the polynomial expressions of the specific heat capacities as functions of temperature are taken from [8] and [9], respectively. For simplicity, we consider here a mixture of N perfect gases; the total pressure is

$$P = \rho \frac{R_u}{W} T, \quad \text{where} \quad \frac{1}{W} = \sum_{k=1}^N \frac{Y_k}{W_k} \quad (11)$$

with W_k being the molar weight of species k . c_p , the heat capacity at constant pressure of the mixture, and c_v , the heat capacity of the mixture at constant volume are defined as

$$c_p = \sum_{k=1}^N c_{pk} Y_k, \quad c_v = \sum_{k=1}^N c_{vk} Y_k \quad (12)$$

In our code we use the semi-empirical formula for diffusion coefficient of the multi-component mixture of Wilke [10]

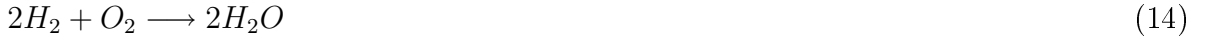
$$\mu = \sum_{k=1}^N \frac{X_k \mu_k}{\sum_{j=1}^N X_j \phi_{ij}}, \quad \text{with} \quad \phi_{ij} = \frac{[1 + (\mu_i/\mu_j)^{1/2} (W_j/W_i)^{1/4}]^2}{(8 + 8W_i/W_j)^{1/2}} \quad (13)$$

This formula is for a mixture of N gases, where W_i are the molecular weights and X_i are the molar fractions. A similar formula is recommended by Wilke for the thermal conductivity λ of a mixture of N gases except that μ_k are replaced by λ_k . The values of μ_k , λ_k and their temperature dependences are taken from [11].

3.2 Combustion model

The combustion model provides the reaction rates $\dot{\omega}_i$ for the premixed gas chemical reaction. The rates appear in the source terms of the energy (4) and the species transport equations

(2). The reaction rates used in this paper are all relying on the global reaction mechanism



The rates of production and destruction of the different species $\dot{\omega}_j$ ($j = H_2, O_2, H_2O$) are given by:

$$\dot{\omega}_{H_2} = -2W_{H_2} \dot{\omega} \quad (15)$$

$$\dot{\omega}_{O_2} = -W_{O_2} \dot{\omega} \quad (16)$$

$$\dot{\omega}_{H_2O} = 2W_{H_2O} \dot{\omega} \quad (17)$$

The reaction rate used in our case is the laminar Arrhenius rate

$$\dot{\omega} = C_f \left(\frac{\rho_{H_2}}{W_{H_2}} \right) \left(\frac{\rho_{O_2}}{W_{O_2}} \right) \exp(-T_a/T) \quad (18)$$

where $C_f = 3.3 \times 10^8 \text{ m}^3/\text{mol/s}$ and T_a is the activation temperature, $T_a = 10^4 \text{ K}$. This choice of parameters would give an experimental value of fundamental flame velocity for stoichiometric hydrogen-air mixture, $S_L = 2.09 \text{ m/s}$.

Quenching Criterion.

The states of flame propagation are closely related to the flame temperature. As the temperature of the flame front decreases to a certain value, flames do not propagate forward due to the weak combustion reaction. This value is called quenching temperature [12]. In the earlier studies [2], [13] it has been the common practice to take for the value or range of values of this quenching temperature the ones close to the maximum flame temperature, while in [14] the quenching temperature T_q is defined as

$$T_q = T_{adiab.} - \frac{T_{adiab.}^2}{T_a}. \quad (19)$$

where $T_{adiab.}$ is the adiabatic temperature. Under the conditions considered here, $T_q = 1817 \text{ K}$.

In this study $\dot{\omega}$ was set equal to zero for temperatures less than the temperature $T_q = 1800\text{K}$, i.e.

$$\dot{\omega}_{quench} = \dot{\omega}H(T - T_q), \quad (20)$$

with H being the Heaviside function.

4 Numerical modelling

The Navier-Stokes equations (1)-(4) are discretised using Finite Volume approach with Shock-Shock approximate Riemann solver for convective terms and ‘‘diamond’’ method for diffusive terms [15].

The sketch of discretised domain is presented on the Fig. 2, where D is the mesh wire diameter taken here to be 0.3 mm . The area painted in red is the ignition region where we assign AIBC (Adiabatic IsoBaric complete Combustion) conditions, i.e. $T_{red} = 2387.7 \text{ K}$ and $P_{red} = 1 \text{ atm}$. Lower and upper boundaries are non-slip and adiabatic while at the cylinder we assume constant temperature and zero fluid velocity.

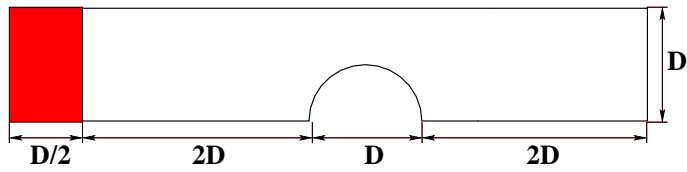
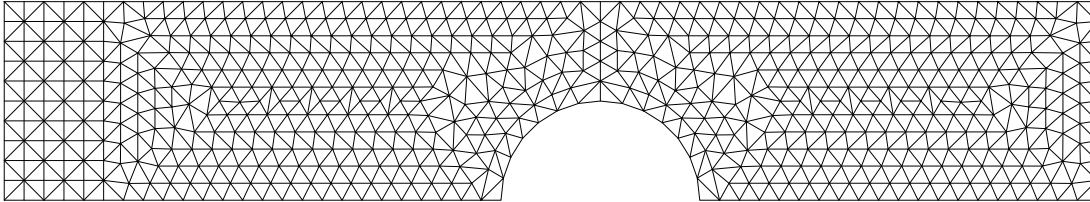
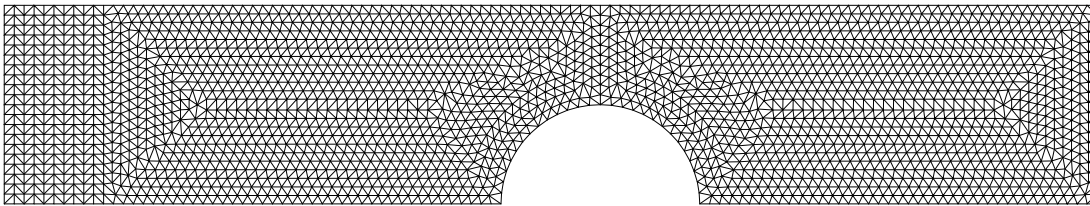


Figure 2: Sketch of discretised domain.

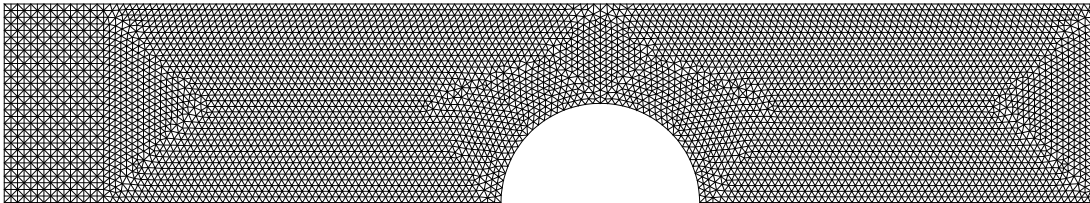
On the Fig. 3 we present numerical grids used for computing a flame quenching: the coarse grid is made of 1134 triangular cells, the medium grid - of 4548 cells, and the fine grid - of 10354 cels. The averaged cell size of each grid computed as



1134 elem., dx=0.02 mm



4548 elem., dx=0.014 mm



10354 elem., dx=0.0092 mm

Figure 3: Numerical grids made of 1134 elements (top), 4548 elements (middle), and 10354 elements (bottom).

$$dx = \sqrt{\frac{V_{tot}}{N_{elem}}} \quad (21)$$

is 0.02 mm, 0.014 mm and 0.0092 mm, respectively. This means that on the fine mesh the laminar flame width δ_L , estimated as $\delta_L = D_{H_2}/S_L$ is represented by at least 4 numerical cells.

We apply an explicit scheme in time with a time step computed as

$$\Delta t = CFL \times \min \left\{ \frac{dx}{|\vec{u}| + c} \right\}, \quad \text{with} \quad c = \sqrt{\frac{\gamma P}{\rho}} \quad \text{and} \quad CFL < 1. \quad (22)$$

5 Numerical Results

We have performed the numerical simulations using three grids presented above for grid sensitivity study.

The computed flame propagation and quenching process can be separated into three phases: **1)** flame initiation and initial propagation during which the flame advances roughly one diameter from the ignition region; **2)** flame propagation towards a cold cylinder; **3)** flame “stagnation” at a fixed position close to the cylinder. We stop the computation when the heat loss to the cylinder has higher value than the heat generated due to combustion.

During the first phase the temperature profile in horizontal direction, having initially a step-function distribution, will be smoothed due to the viscous terms of the Navier-Stokes equations. We have applied the Eq. 18, i.e. Arrhenius expression without the Heaviside function, for this step in order to facilitate the smoothing effect.

The consecutive flame behaviour in terms of temperature distribution at the phases 2) and 3), are shown on the Figs. 4-6. We can see that initially, the effect of cold cylinder on flame propagation is very low. With increasing heat loss at its cold surface, temperature near the surface decreases. The decrease in temperature inevitably weakens the combustion reaction near the cylinder, while the higher temperature region is still formed at the upper boundary. Relatively high numerical viscosity affects the flame propagation (see Fig. 4) - it is quenched before departing the cylinder location at the upper boundary. The temperature distributions computed using medium and fine mesh (Figs. 5-6) have similar structures, i.e. before stagnation the flame in both cases overtakes the cylinder location at the upper part of the domain.

When approaching the cylinder, i.e. during the stagnation phase the energy generated by the flame during a time unit should have the same order of magnitude as the energy lost to the cold cylinder. We shall confirm this statement using the numerical solution corresponding to the three meshes presented above.

On the Fig. 7 the power balance in terms of $\frac{Q_{generated} - Q_{lost}}{Q_{generated}} \times 100\%$ during flame propagation and stagnation phases is presented. During initial times, $t < 1.0 \times 10^{-4}$ s, the rate of heat loss is small, i.e. the power balance is close to 100 %. When the flame approaches the cold cylinder the heat loss per second increases until it becomes bigger than the rate of heat generation.

The presented power balance evolutions are not only the results of contributions of different terms of the Navier-Stokes equations, but also of the numerical viscosity which is present due to approximation of these terms. It is generally accepted that the magnitude of the numerical viscosity diminishes with grid refinement. Thus we can hope that the solutions obtained on the medium and the fine meshes are closer to the physical solution. Interestingly, the power balance evolutions corresponding to these grids show oscillatory behaviour for $t > 0.17$ ms, with an approximate period of 14 μ s. The power balance evolution corresponding to the coarse mesh oscillates with higher frequency; we attribute this behaviour to the influence of relatively excessive numerical viscosity.

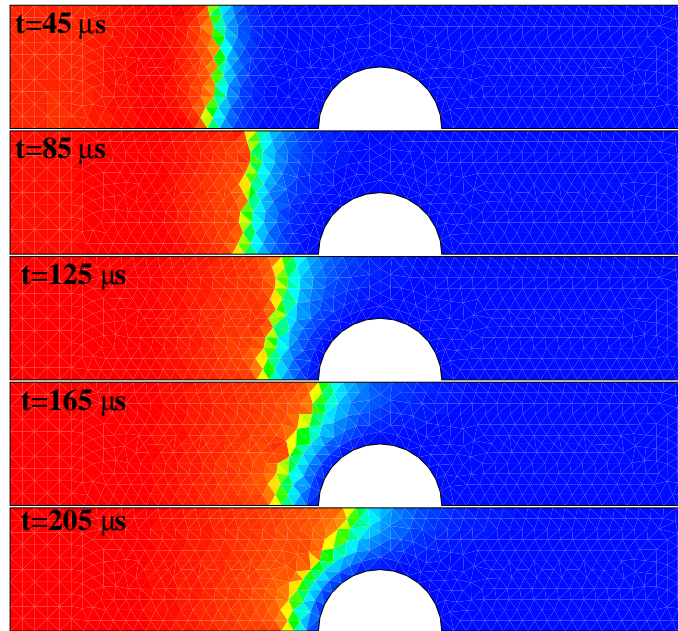


Figure 4: Temperature contours evolutions due to flame propagation. Red color corresponds to burnt gases ($2387K < T < 2520K$), blue color - to fresh gases ($300K < T < 312K$). Coarse mesh.

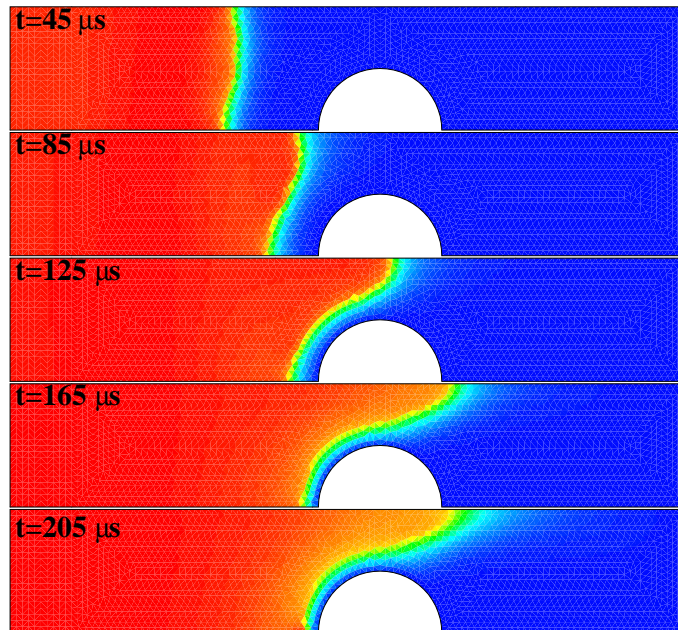


Figure 5: Temperature contours evolutions due to flame propagation. Red color corresponds to burnt gases ($2387K < T < 2520K$), blue color - to fresh gases ($300K < T < 312K$). Medium mesh.

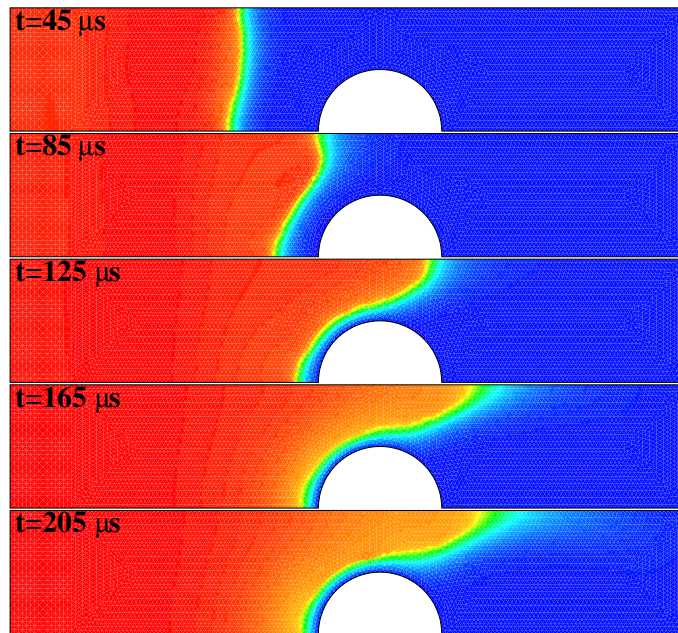


Figure 6: Temperature contours evolutions due to flame propagation. Red color corresponds to burnt gases ($2387K < T < 2520K$), blue color - to fresh gases ($300K < T < 312K$). Fine mesh.

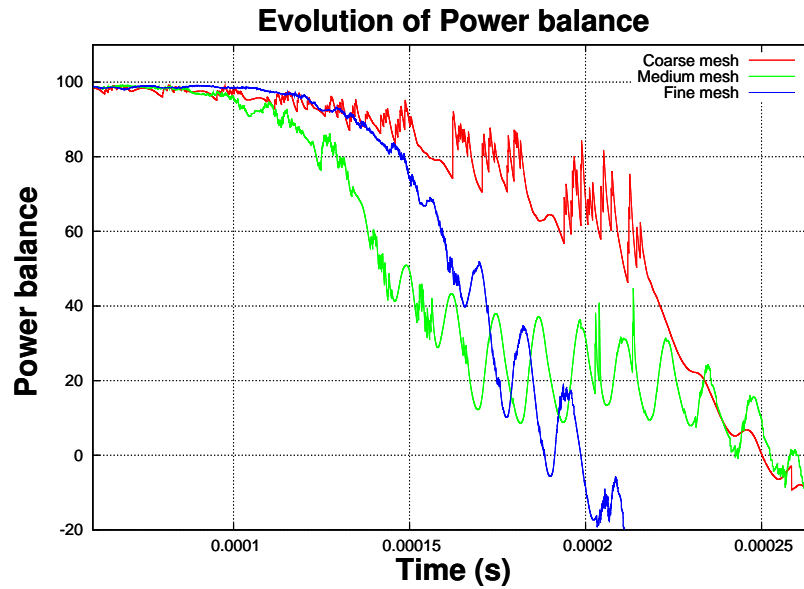


Figure 7: Variation of the power balance with time, $\frac{(Q_{generated} - Q_{lost})}{Q_{generated}} \times 100\%$.

6 Conclusions and Discussions

In view of the results just presented, the following conclusion may be drawn.

- 1) The solution of the two-dimensional equations modeling a laminar flame propagating towards the quenching mesh, provides an interesting insight into the flame quenching mechanism due to the heat loss to the low temperature mesh.
- 2) For comparisons between the various quenching studies, quenching Peclet number is usually used, which is defined as [2]

$$Pe = \frac{S_L D_{quench}}{\alpha}, \quad (23)$$

where S_L , D_{quench} and α are combustion velocity of laminar flame, quenching diameter and thermal diffusivity, respectively. For cold channels and tubes the values of the Peclet number vary from 25.4 to 60 (for references please see [12]). For metallic meshes under the conditions described in this article the value of the Peclet number is about 25 which is in a good agreement with earlier results.

- 3) Physically, there is another reason for cessation of chemical reaction near the cold wall (apart from the low temperature cut-off of the kinetics), namely the recombination of the active radicals during diffusion through the relatively cool region near wall. The authors could not find any references with measurements related to the latter reason, apart from some studies in [3] where some classification of surface materials with respect to chain breaking has been performed. On the modelling side, if one wanted to simulate the effect of wall capture of hot radicals, one could add an appropriate sink terms to the species equations. Obviously, to do this, it would be necessary to consider multi-step reaction mechanism.

- 4) As a future work we would like to suggest the experimental, theoretical and computational studies of the *turbulent* flame quenching phenomenon. From the computational point of view, it will be interesting to characterize not only a thermal effect, by which heat losses to the quenching mesh affect the turbulent flame structure, but also a geometrical effect which limits the spatial extent of the flame brush and affects the flame-brush size in the vicinity of the mesh.

References

- [1] Song, J.H., Kim, S.B., Kim, H.D., On some salient unresolved issues in severe accidents for advanced light water reactors, *Nuclear Engineering and Design*, 235, 2005, pp. 2055-2069.
- [2] Aly, S.L., Hermance, C.E., A two-dimensional theory of laminar flame quenching, *Combustion and Flame*, 40, 1982, pp. 173-185.
- [3] Lewis, B., Von Elbe, G., *Combustion, Flames and Explosions of Gases*, 1987, Academic Press, INC.
- [4] Phillips, H., On the transmission of an explosion through a gap smaller than the quenching distance, *Proc. Roy. Soc.*, 7, 1963, pp.129-135.
- [5] Kim, H.J. et al., A study on quenching meshes as a possible controlling tool of hydrogen explosion in nuclear power plants, ICONE10-22232, Arlington.

- [6] Internet site: <http://www-cast3m.cea.fr>
- [7] Poinso, T., and Veynante, D., *Theoretical and Numerical Combustion*, 2001, Edwards.
- [8] Stull, D.R. and Prophet, H., *JANAF thermochemical data*, U.S. Government Printing Office, Washington, 1971.
- [9] Gardiner, C., *Combustion Chemistry*, 1984, Springer-Verlag.
- [10] White, F.M., *Viscous Fluid Flow*, 1974 Mc Graw-Hill.
- [11] W.M. Rohsenow, J.P. Hartnett and Y.I. Cho, *Handbook of Heat Transfer*, McGraw-Hill Handbooks, 1998.
- [12] Song, Z.B., Duo, Y.Q., Wei, L.J., Wu, Z.Z., Effects of heat losses on flame shape and quenching of premixed flames in narrow channels, *Combust. Sci. and Tech.*, 180, 2008, pp.264-278.
- [13] Aly, S.L., Simpson, R.B., Hermance, C.E., Numerical solution of the two-dimensional premixed laminar flame equations, *AIAA Journal*, 17 No.1, 1979, pp.56-63.
- [14] Zeldovich, Ya.B., Theory of the propagation limit of a quiet flame, *Zh. Exp. Teor. Fiz.*, 11, 1941, pp.159-169.
- [15] Beccantini, A., *Solveurs de Riemann pour des Mélanges de Gas parfaits avec Capacités Calorifiques Dépendant de la Température*, PhD Thesis, 2001, University d'Orsay.